Influence of Ionization State on the Activation of Temocapril by hCES1: A Molecular-Dynamics Study

by **Giulio Vistoli***[a]), **Alessandro Pedretti**[a]), **Angelica Mazzolari**[a]), **Cristiano Bolchi**[a]), and **Bernard Testa**[b])

[a]) Dipartimento di Scienze Farmaceutiche 'Pietro Pratesi', Facoltà di Farmacia, Università degli Studi di Milano, Via Mangiagalli, 25, IT-20133 Milano
(phone: +39 02 19349; fax: +39 02 19359; e-mail: Giulio.Vistoli@unimi.it)
[b]) Department of Pharmacy, University Hospital Centre (CHUV), Rue du Bugnon, CH-1011 Lausanne

Temocapril is a prodrug whose hydrolysis by carboxylesterase 1 (CES1) yields the active ACE inhibitor temocaprilat. This molecular-dynamics (MD) study uses a resolved structure of the human CES1 (hCES1) to investigate some mechanistic details of temocapril hydrolysis. The ionization constants of temocapril (p*K*1 and p*K*3) and temocaprilat (p*K*1, p*K*2, and p*K*3) were determined experimentally and computationally using commercial algorithms. The constants so obtained were in good agreement and revealed that temocapril exists mainly in three ionic forms (a cation, a zwitterion, and an anion), whereas temocaprilat exists in four major ionic forms (a cation, a zwitterion, an anion, and a dianion). All these ionic forms were used as ligands in 5-ns MS simulations. While the cationic and zwitterionic forms of temocapril were involved in an ion-pair bond with Glu255 suggestive of an inhibitor behavior, the anionic form remained in a productive interaction with the catalytic center. As for temocaprilat, its cation appeared trapped by Glu255, while its zwitterion and anion made a slow departure from the catalytic site and a partial egress from the protein. Only its dianion was effectively removed from the catalytic site and attracted to the protein surface by Lys residues. A detailed mechanism of product egress emerges from the simulations.

1. Introduction. – Because metabolic problems lead to many failures during clinical trials, much effort is now devoted to *in silico* models to predict and rationalize metabolic stability and metabolites. Such models are well-known for cytochromes P450 and various conjugating enzymes, and they enjoy a relative success [1][2]. Conversely, little if any has been done to rationalize and predict *in silico* the hydrolyzing activity of the human esterases, although they play key roles in the hydrolytic metabolism of xenobiotics, as well as in the activation of most prodrugs [3][4].

Among the human esterases, carboxylesterases play a pivotal role in the hydrolysis of a variety of drugs or prodrugs containing ester, amide, or carbamate functions to the respective free acids [5][6]. Mammalian carboxylesterases (CESs) are members of the serine hydrolase family (also termed α/β hydrolases) [7]. It has been suggested that CES isozymes can be classified into five subtypes denominated CES1–CES5, even if the majority of the identified CESs belong to the families CES1 or CES2 [8]. The CES1 is known to prefer a substrate with a small alkyl or aryl group and a large acyl group, whereas CES2 recognizes almost exclusively substrates with large alkyl or aryl groups and small acyl groups since its specificity is more constrained by structural hindrances in the active pocket [9].

The inhibitors of the angiotensin-converting enzyme (ACE) are of crucial importance for the treatment of various cardiovascular disorders [10] and represent classical examples of ester-containing prodrugs, since, with the exception of captopril and lisinopril, they require bioactivation by non specific esterases. In particular, temocapril (=(+)-[(2*S*,6*R*)-6-{[(*S*)-1-(ethoxycarbonyl)-3-phenylpropyl]amino}-5-oxo-2-(thiophen-2-yl)-1,4-thiazepan-4-yl]acetic acid), is a zwitterionic orally active, long-acting prodrug-type ACE inhibitor [11]. It is rapidly absorbed and converted exclusively to its pharmacologically active diacid metabolite, temocaprilat (*Fig. 1*), predominantly by carboxylesterases (CES). Hence, human CES enzymes (hCESs) play a central role in the pharmacokinetic profile of temocapril influencing the disposition of both the parent compound and active metabolite. According to the reported substrate specificity of carboxylesterases, it comes as no surprise that

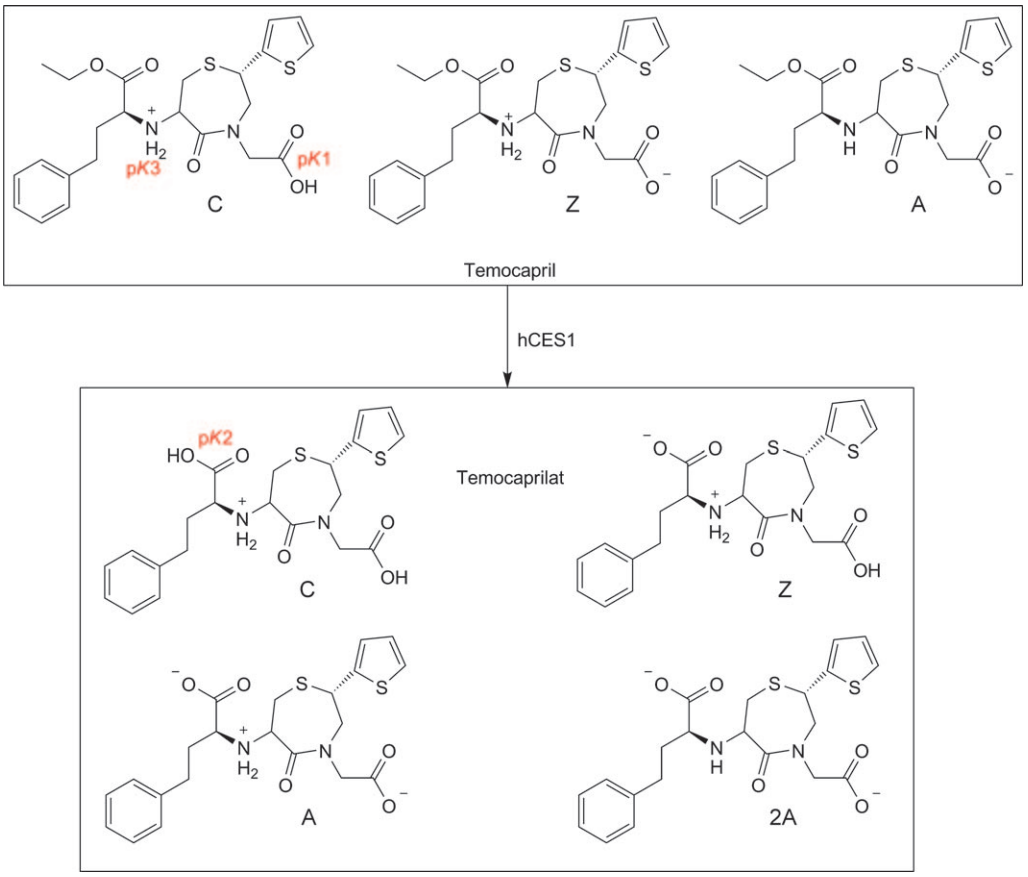

Fig. 1. *The structure of temocapril and its hCES1-catalyzed hydrolysis to the active metabolite temocaprilat*. The *Figure* shows the groups contributing most to p*K*1, p*K*3 and p*K*2, respectively. Also shown are all ionized forms, namely the cations (C), zwitterions (Z), anions (A), and dianion (2A). All these electrical states were considered in the MD simulations.

temocapril is a better substrate of hCES1 than of hCES2, as evidenced by the respective V_{max} values (4.76 *vs.* 0.402 μmol/mg protein/min) [12].

In a previous modeling study of hCES1 biocatalysis [13], we showed that the protonation state of the substrate plays a key role in its recognition by the enzyme and in modulating the efficiency of the catalytic turnover. In particular, the simulations revealed that protonated substrates are bound and trapped in the catalytic pocket by strong ionic bonds. Such a behavior is well explainable considering the numerous negatively charged residues contained in the enzymatic cavity, probably to promote the egress of the (anionic) products. Globally, this fact implies that the local pH in the enzymatic cavity can control which ionizable esters become substrates, since negatively charged compounds are repelled without being hydrolyzed, while positively charged compounds are trapped by strong interactions and behave as inhibitors. To investigate the role of ionization on CES1-catalyzed hydrolysis and further substantiate this hypothesis, we report MD simulations of hCES1 in complex with temocapril and temocaprilat in various states of ionization. Thanks to their basic and acidic groups, these compounds indeed represent excellent probes to analyze how the pH of the enzymatic cavity can influence the behavior of simulated complexes and thus the catalytic efficiency of hCES1.

2. Results. – 2.1. *Ionization Properties of Temocapril and Temocaprilat*. The pK_a values of temocapril (p*K*1 and p*K*3) and temocaprilat (p*K*1, p*K*2, and p*K*3; see *Fig. 1*) were determined experimentally by potentiometric titration and computationally using three softwares, namely *Molecular Discovers*'s MoKA [14], the *ACD* package [15], and VCCLAB from *Pharma Algorithm* [16]. The p*K* values (*Table 1*) reveal that the basicity of the amino group (p*K*3) is increased over 100-fold following temocapril hydrolysis to temocaprilat. In contrast, the acidity of the carboxylate function in position 4 (p*K*1) is not affected by the hydrolysis of the ester group. In temocaprilat, the highly acidic carboxylic function α to the amino group (p*K*2) strongly increases the basicity of the latter, from 4.61 to 6.95. As a result, the amino group in temocapril is essentially unprotonated at physiological pH, whereas it is mostly protonated in temocaprilat. Interestingly, the total charge in the ionic form predominating at physiological pH is the same (*i.e.*, -1) in both compounds. The values predicted by the three algorithms for these difficult molecules are in good agreement with experimental

Table 1. *Computed and Experimental Ionization Constants of Temocapril and Temocaprilat*[a])

Ionization constant	Computed			Average of computed values	Experimental values
	by MoKA	by *ACD*	by VCCLAB		
Temocapril p*K*1	3.21	3.73	3.10	3.35 ± 0.34	2.76 ± 0.01
Temocapril p*K*3	5.51	4.49	5.50	5.12 ± 0.58	4.61 ± 0.02
Temocaprilat p*K*1	3.21	3.73	3.10	3.35 ± 0.34	3.67 ± 0.04
Temocaprilat p*K*2	2.25	2.09	2.30	2.22 ± 0.11	1.81 ± 0.29
Temocaprilat p*K*3	7.64	6.86	8.20	7.57 ± 0.67	6.95 ± 0.04

[a]) See *Fig. 1* for the definition of p*K*1, p*K*3, and p*K*2, and the *Exper. Part* for the algorithms and instrument used.

data, the mean calculated for 15 differences (in absolute values) being 0.53 ± 0.20. Of particular interest is the fact that increase in basicity (p*K*3) from prodrug to metabolite is correctly accounted for.

As depicted in *Fig. 1*, the predicted p*K* values allow the definition of the major electrical forms, namely three ionization states for temocapril (termed as C = cation, Z = zwitterion, and A = anion), and four states for temocaprilat (termed as C = cation, Z = zwitterion, A = anion, and 2A = dianion). All these ionization states were taken into account by the MD simulations.

2.2. *MD Simulations of Temocapril Ionic Forms Complexed with CES1.* The complex between CES1 and temocapril confirms that the labile ester function is able to approach the catalytic Ser221 residue, while the ligand arranges its hydrophobic/aromatic moieties to optimize their apolar contacts. Indeed, the phenyl ring is involved in $\pi-\pi$ interactions with Phe426 and His468, while the thiazepane and thiophene rings contact a large set of aliphatic residues including Met145, Leu255, Leu304, Leu318, Leu358, Ile359, Leu363, and Met364. The thiophene ring is also involved in a $\pi-\pi$ interaction with Phe303. Globally, this interaction pattern emphasizes the critical role of hydrophobic interactions and can explain the preference of CES1 for lipophilic substrates as well as its substrate promiscuity, given the low directional specificity of such interactions and the absence of polar contacts apart with Ser221.

Fig. 2 depicts the stability of the complexes for the three ionic states of temocapril, as assessed by the distance between Ser221 and the carbonyl C-atom in the ester group. The results show that the complex remained stable in all simulations and was not markedly affected by the ionization state of the ligand. This suggests that the recognition of the substrate is not markedly influenced by its ionization state, even if the anionic form shows a distance sensibly greater than that of the other two states (*Table 2*).

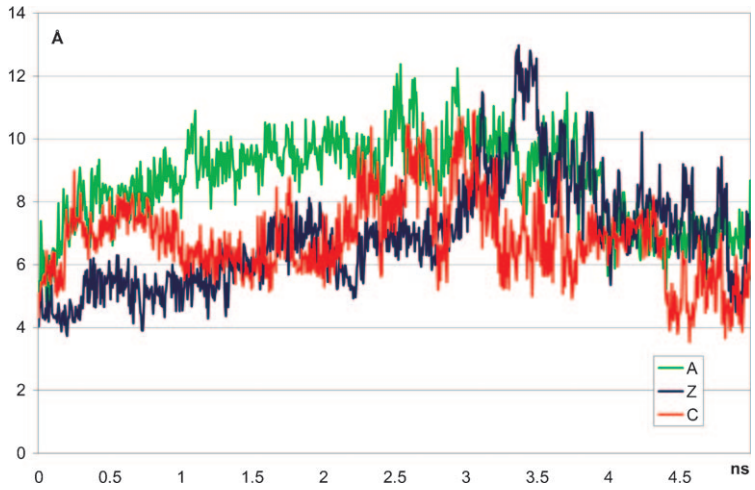

Fig. 2. *Dynamic Profile of the Distance between Ser221 and the ester carbonyl C-atom for the three ionic forms of temocapril* (the color code: red = cation; blue = zwitterion, and green = anion).

Table 2. *Ligand Mobility Derived from MD Simulations and Expressed by the Distance between Ser221* (mean values and final values at 5 ns), *and the Carbonyl C-Atom of the Ester Group* (temocapril) *or of the New Carboxylate Group* (p*K*2, in temocaprilat). Also reported are the mean values of the distance between Lys257 and the carboxylate group corresponding to p*K*1. All values are expressed in Å.

Ionic form considered	Mean distance [Å] to Ser221	Distance [Å] to Ser221 after 5 ns	Mean distance [Å] to Lys257
Temocapril C	6.81	5.53	8.78
Temocapril Z	6.73	7.38	8.66
Temocapril A	8.75	6.62	6.45
Temocaprilat C	8.11	11.70	8.89
Temocaprilat Z	16.68	19.03	5.95
Temocaprilat A	14.96	17.35	4.97
Temocaprilat 2A	19.73	25.71	12.33

A careful comparison of the trajectories for the three ionic forms of temocapril allows to better rationalize their slight differences as seen in *Fig. 2*. Indeed, the interaction pattern that temocapril assumes within the catalytic pocket is somewhat influenced by two long-range ionic contacts with Glu225 (on the side of the catalytic Ser221 residue) and with Lys257 (located on the opposite side toward the pocket entrance). This means that the ionic forms of the substrate which can interact with Glu225 reinforce the complex stability, whereas the forms which can form ion pairs with Lys257 alter the binding mode of the substrate and move it toward the exit. On these grounds, the practically superimposable profiles of the cationic and zwitterionic forms are easy to understand, considering that in both states the ionic contacts with Glu225 guarantee an effective complex stability. Similarly, the greater distance of the anionic form may be due to interconverting interactions with Ser221 and Lys257; in the latter case, the ionic bond is no longer counteracted by an electrostatic interaction with Glu225, as confirmed by the lower distance between the carboxylate function and Lys257 (*Table 2*). Nevertheless, the destabilizing interaction with Lys257 is counterbalanced by a catalytic contact with Ser221 which prevents egress of the ligand.

2.3. *MD Simulations of Temocaprilat Ionic Forms Complexed with CES1.* The simulations with the ionic forms of temocaprilat reveal a markedly less homogeneous behavior than observed with temocapril, demonstrating that, in this case, the product egress is significantly affected by its ionization state. *Fig. 3* shows the dynamic profile for the monitored distance between Ser221 and the free carboxylic group (p*K*2) for the four ionic forms of temocaprilat and reveals three distinct behavior patterns. First, the dianionic form (2A) rapidly exits the enzymatic pocket, an effect compatible with an efficient catalytic turnover. Second, the cationic form (C) remains fully entrapped in the catalytic site and behaves as an inhibitor. Third, the zwitterionic and monoanionic forms (Z and A) display an intermediate behavior, since they move away from Ser221 but more slowly than the dianionic form. This result confirms that a basic protonated group is detrimental for product mobility irrespective of its total charge, an observation explained by the numerous negatively charged residues which line the catalytic channel.

A careful analysis of the simulations emphasizes the key role of some lysine residues (*e.g.*, Lys92, Lys257, and Lys302). Indeed, their role is postulated to facilitate

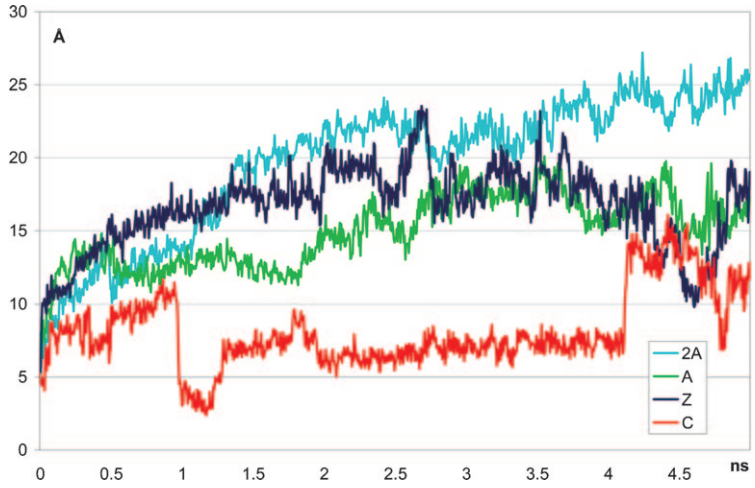

Fig. 3. *Dynamic profile of the distance between Ser221 and the carbonyl C-atom of the new carboxylic group* (p*K*2) *for the four major ionic forms of temocaprilat* (the color code: red = cation; blue = zwitterion, green = anion, and cyan = dianion).

the egress of the dianionic product by first attracting it away from the catalytic (this would be the role of Lys257 located in the middle of the exit pathway), and then by attracting it to the protein surface (the postulated role of Lys92 and Lys302 located at the end of the exit channel and facing the protein surface).

Considering the key residues lining the exit pathway and examining the simulated trajectories, one sees that the exit process of temocaprilat occurs in three steps as schematized in *Fig. 4*. In the first step, the product is no longer retained by Ser221 and is induced by Lys257 to leave the catalytic site. In the second step, the interaction with Lys257 allows the product to rotate so that its other carboxylate group is turned toward the channel exit. Lastly, the product breaks contact with Lys257 and reaches the protein surface due to the attraction by Lys92 and Lys302. Clearly, this exit mechanism may not be valid for all CES1 substrates and is probably quite specific for dianionic temocaprilat. Thus, its cationic form does not feel the attraction of lysine residues, since its protonated amino group traps the product into the catalytic site where it would behave as an inhibitor. The monoanionic and zwitterionic forms leave the catalytic site but remain anchored to Lys257. In other words, they undergo the first two steps of the egress mechanism but fail to complete the third. Indeed, the rotation of the product mediated by Lys257 occurs even when the second carboxylic group (p*K*1) is neutral, although the monoanionic form shows a smaller mobility than the zwitterionic form. As stated, only the dianionic state can complete the product egress by contacting Lys92 and Lys302, and reaching the protein surface. This observation also confirms that a protonated group hampers the product exit irrespective of the ionization of the carboxylic groups, probably due to strong polar interactions with residues near Lys257, for example, with Ser305, or it is repelled by the positively charged Lys92 and Lys302. One expects that longer MD simulations would allow the monoanionic and zwitterionic

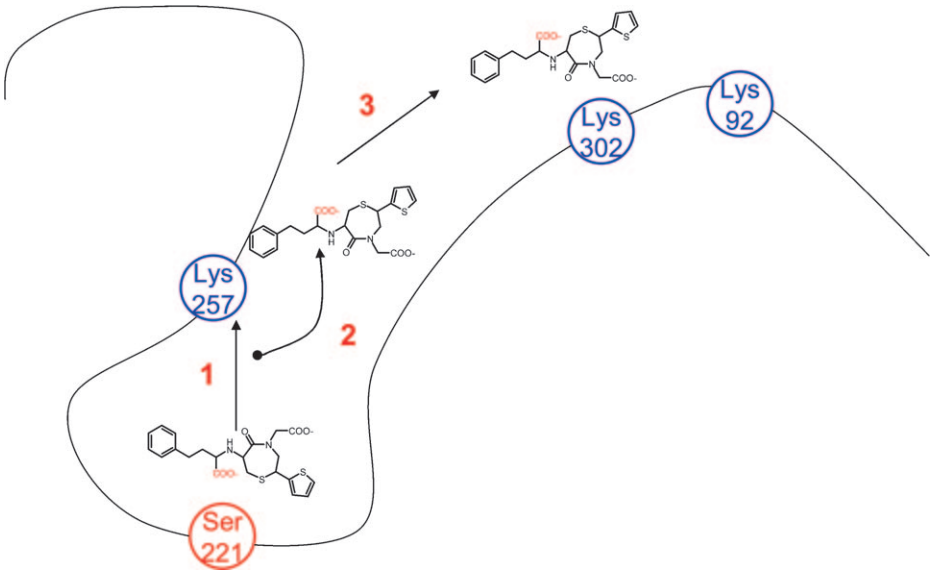

Fig. 4. *Schematic representation for the three-step mechanism for the egress pathway of temocaprilat as observed in MD simulations.* One can note that, in the first step, the ligand leaves the catalytic center due to attraction by Lys257, in the second step it rotates around Lys257 directing the free carboxylate group toward the exit, and finally it leaves Lys257 and approaches the enzyme surface.

forms to complete the exit pathway. Yet, the present simulations suggest that the dianionic state should have the fastest egress, thereby enhancing the catalytic turnover.

Globally, the present simulations indicate that the catalytic pocket of hCES1 should have a well-defined microenvironment to optimize its catalytic activity. The results suggest that such a microenvironment should be rather basic to accelerate the hydrolysis of temocapril, but the enzyme may also undergo conformational rearrangement in side chains to maximize its efficiency toward a given substrate. The modest catalytic parameters of temocapril hydrolysis, despite the many hydrophobic contacts that stabilize its complex with CES1, suggest that the micro-pH of the catalytic pocket is not truly optimal for this substrate.

3. Conclusions. – In the present work, we investigated a feature of ligand recognition often disregarded by traditional modeling studies, since it exploits MD simulations to analyze how ionization states can influence substrate recognition and product egress, two major components of enzymatic efficiency. The interest in such a study is twofold. First, it can suggest the probable micro-pH of the enzymatic milieu to ensure a productive binding mode of the substrate, and a complete and fast egress of the metabolite. Second, the study can offer new insights into the scarce reactivity of some ionizable substrates, especially when large differences between the ionization properties of the substrate and its product prevent the occurrence of an optimal micro-pH allowing both optimal substrate recognition and quick product egress.

Moreover, the study confirms that the protonated amino group in temocapril can have detrimental effects on CES1 activity, because it alters its binding mode and prevent product egress, which appears to be fully effective only for the dianionic form. Finally, the study suggests a detailed mechanism for the exit pathway. Even supposing that this mechanism is specific for temocaprilat, it affords relevant information on the role of key residues in producing a productive binding mode of the substrate and guiding product egress; the mechanism might even be of value in designing non-competitive inhibitors which bind far from the catalytic center.

The authors are indebted to Prof. *Gabriele Cruciani*, University of Perugia, for the calculation of the pK_a values of temocapril and temocaprilat using the MoKA algorithm.

Experimental Part

1. *Determination of the p*K$_a$ *Values of Temocapril and Temocaprilat.* Temocapril was purchased from *Novachimica* (Italy). Temocaprilat was then prepared by hydrolysis in aq. NaOH as described in [11]. Their ionization constants were determined at 25° by potentiometric titration using the *Sirius GlPKa* apparatus (*Sirius Analytical Instruments Ltd.*, Forest Row, East Sussex, U.K.). All experiments were carried out under a slow N_2 flow to avoid CO_2 absorption. A weighted sample (2–10 mg) was supplied manually; the diluent and all the other reagents were added automatically. Specifically, the compounds were solubilized in 0.15M KCl (to adjust ionic strength) and acidified with 0.1M HCl to pH 1.8. The solns. were then titrated with normalized KOH to pH 12.2. *Bjerrum*-difference plots were deduced from each titration and used to calculate precise p*K* values. The detailed exper. procedures and data analyses as well as the recommended apparatus standardization can be found in [17].

2. *Preparation of the Simulated Complexes.* The docking analyses performed in the previous study [13] involved different X-ray structures and showed that the best predictive simulations were carried out using the resolved structure in complex with benzoate (PDB Id: 1YAJ), an enzymatic product which is derived from degradation of the benzil inhibitor (1,2-diphenylethane-1,2-dione) a *retro*-aldol condensation, followed by hydrolysis [18]. Therefore, this resolved structure was also used in the present study to simulate the enzymatic complexes with temocapril and temocaprilat. In fact, the starting complex of hCES1 with the anionic form of temocapril was taken from docking results of the previous study [13]. Briefly, the complex was generated using *OpenEye Scientific* Software package FRED, focusing the sampling on a 10-Å side box around Ser221, which is the residue of the catalytic triad contacting the substrate's hydrolyzable group. The resulting complex was minimized keeping fixed all atoms outside a 15-Å radius sphere around the bound substrate to favor the mutual adaptability between ligand and enzyme. This complex was then manually modified to generate both the complexes with the other ionization states of temocapril as well as all simulated states for temocaprilat. Such modified complexes were finally minimized keeping fixed all atoms outside a 15-Å radius sphere around the bound ligand.

3. *MD Simulations.* MD Simulations involved hCES1 in complex with temocapril and temocaprilat considering their major ionic forms as depicted in *Fig. 1*. Specifically, the forms considered were its cation (C), zwitterion (Z), and anion (A) for temocapril, and its cation (C), zwitterion (Z), anion (A), and dianion (2A) for temocaprilat.

The seven complexes were inserted in a 50-Å radius sphere of H_2O molecules (*ca.* 10000 H_2O molecules); after a preliminary minimization to optimize the relative position of solvent molecules, the systems underwent 5 ns of all-atoms MD simulations with the following characteristics: *a*) spherical boundary conditions were introduced to stabilize the simulation space; *b*) *Newton*'s equation was integrated using the r-RESPA method (every 4 fs for long-range electrostatic forces, 2 fs for short-range nonbonded forces, and 1 fs for bonded forces); *c*) the temp. was maintained 300 ± 10 K by means of *Langevin*'s algorithm; *d*) *Lennard–Jones* (*L-J*) interactions were calculated with a cut-off of 10 Å, and the pair list was updated every 20 iterations; *e*) a frame was stored every 5 ps, yielding 1000 frames; *f*) no constraints were applied to the systems.

The simulations were carried out in two phases: an initial period of heating from 0 to 300 K over 6000 iterations (6 ps, *i.e.*, 1 K/20 iterations), and a monitored phase of simulation of 5 ns. Only those frames memorized during this last phase were considered. The calculations described here were carried out on a 16 CPU Tyan-VX50 system using Namd2.6 [19] with the force field CHARMM and *Gasteiger*'s atomic charges.

REFERENCES

[1] B. Testa, S. D. Krämer, *Chem. Biodiversity* **2006**, *3*, 1053.
[2] P. Czodrowski, J. M. Kriegl, S. Scheuerer, T. Fox, *Exp. Opin. Drug Metab. Toxicol.* **2009**, *5*, 15.
[3] P. Ettmayer, G. L. Amidon, B. Clement, B. Testa, *J. Med. Chem.* **2004**, *47*, 2393.
[4] J. M. Hatfield, M. Wierdl, R. M. Wadkins, P. M. Potter, *Exp. Opin. Drug Metab. Toxicol.* **2008**, *4*, 1153.
[5] T. Imai, *Drug Metab. Pharmacokinet.* **2006**, *21*, 173.
[6] M. Hosokawa, *Molecules* **2008**, *13*, 412.
[7] B. Testa, S. D. Krämer, *Chem. Biodiversity* **2007**, *4*, 2031.
[8] T. Satoh, M. Hosokawa, *Annu. Rev. Pharmacol. Toxicol.* **1998**, *38*, 257.
[9] T. Satoh, M. Hosokawa, *Chem. Biol. Interact.* **2006**, *162*, 195.
[10] B. S. Heran, M. M. Wong, I. K. Heran, J. M. Wright, *Cochrane Database Syst. Rev.* **2008**, CD003823.
[11] H. Yanagisawa, S. Ishihara, A. Ando, T. Kanazaki, S. Miyamoto, H. Koike, Y. Iijima, K. Oizumi, Y. Matsushita, T. Hata, *J. Med. Chem.* **1988**, *31*, 422.
[12] S. Takai, A. Matsuda, Y. Usami, T. Adachi, T. Sugiyama, Y. Katagiri, M. Tatematsu, K. Hirano, *Biol. Pharm. Bull.* **1997**, *20*, 869.
[13] G. Vistoli, A. Pedretti, A. Mazzolari, B. Testa, *Bioorg. Med. Chem.* **2009**, in press, doi: 10.1016/j.bmc.2009.10.052.
[14] F. Milletti, L. Storchi, G. Sforna, G. Cruciani, *J. Chem. Inf. Model.* **2007**, *47*, 2172.
[15] M. Meloun, S. Bordovska, *Anal. Bioanal. Chem.* **2007**, *389*, 1267.
[16] I. V. Tetko, J. Gasteiger, R. Todeschini, A. Mauri, D. Livingstone, P. Ertl, V. A. Palyulin, E. V. Radchenko, N. S. Zefirov, A. S. Makarenko, V. Y. Tanchuk, V. V. Prokopenko, *J. Comput.-Aided Mol. Des.* **2005**, *19*, 453.
[17] A. Avdeef, *J. Pharm. Sci.* **1993**, *82*, 183.
[18] C. D. Fleming, S. Bencharit, C. C. Edwards, J. L. Hyatt, L. Tsurkan, F. Bai, C. Fraga, C. L. Morton, E. L. Howard-Williams, P. M. Potter, M. R. Redinbo, *J. Mol. Biol.* **2005**, *352*, 165.
[19] J. C. Phillips, R. Braun, W. Wang, J. Gumbart, E. Tajkhorshid, E. Villa, C. Chipot, R. D. Skeel, L. Kalé, K. Schulten, *J. Comput. Chem.* **2005**, *16*, 1781.

Received May 2, 2009